

Prediction of Prostate-Specific Antigen Recurrence in Men with Long-term Follow-up Postprostatectomy Using Quantitative Nuclear Morphometry

Robert W. Veltri,¹ M. Craig Miller,² Sumit Isharwal,¹ Cameron Marlow,¹ Danil V. Makarov,¹ and Alan W. Partin¹

¹The James Buchanan Brady Urological Institute, The Johns Hopkins University School of Medicine, Baltimore, Maryland and ²Quakertown, Pennsylvania

Abstract

Background: Nuclear morphometric signatures can be calculated using nuclear size, shape, DNA content, and chromatin texture descriptors [nuclear morphometric descriptor (NMD)]. We evaluated the use of a patient-specific quantitative nuclear grade (QNG) alone and in combination with routine pathologic features to predict biochemical [prostate-specific antigen (PSA)] recurrence-free survival in patients with prostate cancer.

Methods: The National Cancer Institute Cooperative Prostate Cancer Tissue Resource (NCI-CPCTR) tissue microarray was prepared from radical prostatectomy cases treated in 1991 to 1992. We assessed 112 cases (72 nonrecurrences and 40 PSA recurrences) with long-term follow-up. Images of Feulgen DNA-stained nuclei were captured and the NMDs were calculated using the AutoCyte system. Multivariate logistic regression was used to calculate QNG and pathology-based solutions for prediction of PSA recurrence. Kaplan-Meier survival curves and predictive probability graphs were generated.

Results: A QNG signature using the variance of 14 NMDs yielded an area under the receiver operator characteristic curve (AUC-ROC) of 80% with a sensitivity, specificity, and accuracy of 75% at a predictive probability threshold of ≥ 0.39 . A pathology model using the pathologic stage and Gleason score yielded an AUC-ROC of 67% with a sensitivity, specificity, and accuracy of 70%, 50%, and 57%, respectively, at a predictive probability threshold of ≥ 0.35 . Combining QNG, pathologic stage, and Gleason score yielded a model with an AUC-ROC of 81% with a sensitivity, specificity, and accuracy of 75%, 78%, and 77%, respectively, at a predictive probability threshold of ≥ 0.34 .

Conclusions: PSA recurrence is more accurately predicted using the QNG signature compared with routine pathology information alone. Inclusion of a morphometry signature, routine pathology, and new biomarkers should improve the prognostic value of information collected at surgery. (Cancer Epidemiol Biomarkers Prev 2008;17(1):102–10)

Introduction

An improved insight into the pelvic anatomy (1) has enabled improvements in surgery and removal of prostate cancer while substantially reducing perioperative complications such as incontinence and impotency (2). Nearly ~30% to 40% of men undergoing definitive treatment for clinically localized prostate cancer report an isolated increase in prostate-specific antigen (PSA) levels with long-term follow-up (3–11). In a series of nearly 2,000 patients treated with prostatectomy at Johns Hopkins Hospital, 304 men developed PSA recurrence (15%) and were monitored without hormone therapy until demonstration of metastasis (3). Of these men, 34% developed distant metastases over a median period of 8 years from the time of the first postoperative PSA

elevation. Pound et al. (3) developed an algorithm to predict actuarial metastasis-free survival that combined Gleason sum score and a PSA time-dependent doubling time derivative. Additionally, Han et al. (4) updated this study cohort and reported on 360 recurrences (17%) of 2,091 men with prostate cancer and they used three preoperative or postoperative variables to create nomograms to assess biochemical recurrence-free survival probabilities. This study found that the overall actuarial PSA-free survival probabilities at 5, 10, and 15 years were 84%, 72% and 61%, respectively, for the study group. Although not commented upon in these particular studies, it may be likely that many patients in the current era of serologic monitoring are more likely to have undetectable asymptomatic radiographic bone lesions as their initial presentation of bone metastases.

In the search of new biomarkers to predict the prognosis of men with prostate cancer, numerous potential serologic and histologic biomarkers have been evaluated, and more are in developmental stages (12, 13). At the tissue level, DNA alterations measured using semiautomated, computer-assisted image cytometry (14–16) or cytogenetics (17) detect abnormal DNA content representing large-scale chromosomal alterations (i.e., tetraploidy, aneuploidy, hyperploidy, etc.) and reflecting

Received 2/23/07; revised 10/3/07; accepted 10/31/07.

Grant support: The Johns Hopkins University Prostate Cancer Specialized Programs of Research Excellence grant P50CA58236, Early Detection Research Network NCI/NIH grant CA08623-06, Prostate Cancer Foundation, and the Patana Fund.

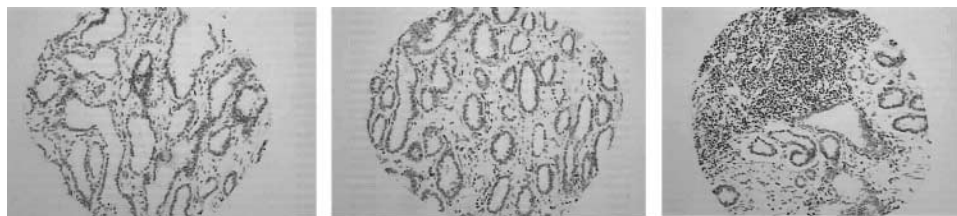
The costs of publication of this article were defrayed in part by the payment of page charges. This article must therefore be hereby marked *advertisement* in accordance with 18 U.S.C. Section 1734 solely to indicate this fact.

Requests for reprints: Robert W. Veltri, James Buchanan Brady Urological Institute, The Johns Hopkins University School of Medicine, Baltimore, MD 21287. Phone: 410-614-6380; Fax: 410-614-3695. E-mail: rveltri1@jhmi.edu

Copyright © 2008 American Association for Cancer Research.

doi:10.1158/1055-9965.EPI-07-0175

Figure 1. Examples of Feulgen DNA-stained CPCTR-TMA cores.



later-stage changes of genetic instability in tumor cells (18). Also, quantitative nuclear morphometry changes (i.e., information on nuclear phenotypic changes) can be derived from Feulgen DNA-stained nuclear images analyzed using computer-assisted image analysis (15, 16, 19). Numerous nuclear morphometric descriptors (NMD) can be calculated based on pixel intensity, density, and distribution patterns from these nuclear images (15, 19). NMDs quantitatively assess nuclear size, shape, DNA content, and chromatin organization (i.e., texture) variables in cancer and adjacent benign areas. Our group has developed methods for calculating quantitative nuclear grade (QNG) solutions to permit the prediction of clinical, diagnostic, and prognostic outcomes in both prostate cancer and bladder carcinoma (15, 19). The current study uses a National Cancer Institute Cooperative Prostate Cancer Tissue Resource (NCI-CPCTR) tissue microarray (TMA) to assess the ability of both available pathology and a QNG signature to predict, at the time of surgery, PSA recurrence and recurrence-free survival times in 112 men with long-term follow-up after radical prostatectomy.

Materials and Methods

Prostate Tissue Specimens Data Set. The CPCTR-TMA is the result of a project funded by a NCI Requests for Application released in April 2000 and four academic institutions [George Washington University Medical Center (Washington DC); Medical College of Wisconsin (Milwaukee, WI); New York University School of Medicine (New York, NY); and the University of Pittsburgh (Pittsburgh, PA)] were funded to form a national prostate cancer tissue resource, the CPCTR. The resource is entirely funded by an individual Cooperative Agreement Grant from the NCI to each of the four participating sites (20, 21). The CPCTR resource functions as a consortium or “virtual tissue bank” with a central database with all four participating sites working jointly with the NCI. Additionally, the methods for TMA construction use a standardized protocol, a database containing standardized common data elements, and a supporting bioinformatics database with outcome results are also provided in a manuscript (22). Additionally, an NCI-CPCTR Web site³ contains information about the project and how to obtain these bioreagents, and for queries regarding these TMAs, one can go to the listserver.⁴

NCI-CPCTR Patient Cohort. Pathologic material from a total of 299 prostate cancer chronologically consecutive radical prostatectomy patients were arrayed over four blocks with a single focus of tumor from each patient tumor represented in duplicate 0.6-mm core spots. For determination of PSA recurrence, an algorithm was applied, and the PSA values needed to increase above 0.6 ng/dL (single value) or have a value between 0.4 and 0.6 ng/dL and show a continued increase in the subsequent PSA values (23). In the latter situation, the PSA recurrence data were calculated based on the initial elevated PSA value above 0.4 ng/dL. A total of 112 prostate cancer cases ($n = 72$ nonrecurrence and $n = 40$

Table 1. Nuclear morphometric descriptors

AutoCyte QUIC-DNA morphometric measurement	Measurement type
Perimeter	Size/shape
Area	Size/shape
Circular form factor	Size/shape
Feret X	Size/shape
Feret Y	Size/shape
Minimum Feret	Size/shape
Maximum Feret	Size/shape
Excess of Gray values	DNA content
Skewness of Gray values	DNA content
SD of Gray values	DNA content
Maximum Gray value	DNA content
Minimum Gray value	DNA content
Intensity	DNA content
Minimum OD	DNA content
Maximum OD	DNA content
Median OD	DNA content
SD OD	DNA content
Skewness of OD	DNA content
Excess of OD	DNA content
DNA ploidy	DNA content
Transmission	Texture
Variance	Texture
Sum average-AC	Texture
Sum entropy-AC	Texture
Sum variance-AC	Texture
Cluster shade	Texture
Diagonal moment-AC	Texture
Sum of homogeneity	Texture
Correlation	Markovian
Difference moment	Markovian
Inverse difference moment	Markovian
Sum entropy-M	Markovian
Entropy	Markovian
Information measure A	Markovian
Information measure B	Markovian
Maximal correlation coefficient	Markovian
Coefficient of variation	Markovian
Peak transition probability	Markovian
Diagonal moment-M	Markovian
Second diagonal moment	Markovian

³ <http://cpctr.cancer.gov>

⁴ ask-cpctr-l@nci.nih.gov

recurrence) from this TMA contained complete information. A notable weakness for this study was the fact that only 36 of 112 prostate cancer (32%) cases had a preoperative PSA level and no longitudinal PSA data were available for PSA kinetic analysis.

QNG Determination. The methods of QNG calculation have been previously reported (16, 19). Using ~5- μ m sections prepared from the TMA blocks, Feulgen DNA staining was done per manufacturer's instructions (TriPath Imaging, Inc.). Next, a minimum of 125 intact, Feulgen DNA-stained cancer nuclei (Fig. 1) were captured from the 0.6-mm spots for each case on the TMA slides using an AutoCyte Pathology Workstation (TriPath Imaging, Inc.) and the QUIC-DNA software (15, 16, 19). The QUIC-DNA software calculated a total of 40 NMDs, including nuclear size, shape, DNA content, and chromatin texture features (at a step size of one pixel), for each nuclei captured (Table 1). For each case, the variance of each NMD was then determined, thereby reducing the complexity of the database to a single set of 40 variables for each case (15, 16, 19). We applied backward stepwise logistic regression to select the multivariately significant NMDs for the differentiation of men with and without prostate cancer recurrence.

Statistical Analysis. All data were analyzed using Stata v9.1 statistical analysis software (Stata Corporation). A nonparametric k -sample χ^2 test for the equality of medians was used to evaluate differences in the nonnormally distributed ages. Wilcoxon's rank sum test was used to test for distribution differences, and Fisher's exact test was used to test for differences in proportions between patients with and without biochemical recurrence in the pathologic stage, Gleason scores, and race. We applied backward stepwise multivariate logistic regression analyses with a stringency level of $P_z < 0.15$ to construct predictive models and calculated areas under the receiver operator characteristic curves (AUC-ROC), sensitivities, specificities, and accuracies for the differentiation of the two groups of men [biochemical (PSA) recurrence]. Using the variable coefficients and constant for each model, patient-specific predictive probabilities were calculated for each case. Plots of the patient-specific predictive probabilities from each model were generated to compare results between the two PSA recurrence groups. The thresholds for the predictive probabilities in each model were selected to provide similar sensitivity and specificity values. Kaplan-Meier survival plots were also created to show the ability of the QNG signature and routine pathologic variables, both separately and in combination, to predict PSA recurrence-free survival. Cox proportional hazards regression was also used to determine the hazards ratios for each model in the determination of PSA recurrence-free survival.

Results

The differences between the two groups for the demographic and pathologic data are shown in Table 2. Noticeable is the absence of serum PSA results for the cohort, as this variable was not available for the majority of the cases in this series from the NCI-CPCTR database.

Applying backward stepwise multivariate logistic regression analysis and a variable selection cutoff of $P_z < 0.05$ to the variance of the 40 NMDs for each case resulted in a QNG signature able to differentiate between recurrence and nonrecurrence of prostate cancer as shown in Table 3 and Fig. 2A and B. This QNG signature used 14 nuclear size, shape, DNA content, and chromatin texture features (NMDs) to calculate patient-specific predictive probabilities (Table 3) and resulted in an AUC-ROC of 80% (Fig. 2A). At a cutoff of 0.39 for the predictive probabilities, the sensitivity, specificity, and accuracy of the model were all 75% (Fisher's exact $P < 0.001$). Figure 2B shows a scatter plot of the patient-specific QNG model predictive probabilities for patients with and without biochemical recurrence.

The results of a backward stepwise multivariate logistic regression model using the pathology variables (i.e., the Gleason score and pathologic stage) and a variable selection cutoff of $P_z < 0.15$ to differentiate between recurrence and nonrecurrence are shown in Fig. 3A and B. The pathology model yielded an AUC-ROC of 67% (Fig. 3A). At a cutoff of 0.35 for the predictive probabilities, the sensitivity, specificity, and accuracy of the model were 70%, 50%, and 57%, respectively (Fisher's exact $P = 0.048$). Figure 3B shows a scatter plot of the patient-specific pathology model predictive probabilities for patients with and without biochemical recurrence. When compared with the QNG signature, the AUC-ROC of the routine pathology model was significantly smaller (80% versus 67%, respectively, $\chi^2 P = 0.0260$).

The results of a multivariate logistic regression model combining the QNG signature and pathology (i.e., the Gleason score and pathologic stage) were shown in Fig. 4A and B. The combined model, which used the QNG signature, the Gleason score, and the pathologic stage, had an AUC-ROC of 81% (Fig. 4A). At a cutoff

Table 2. Prostate cancer patient demographics (n = 112)

Variable description	No biochemical recurrence (n = 72)	Biochemical recurrence (n = 40)	P
Median age, y (range)	66 (47-78)	64 (42-70)	0.107*
Gleason score			
5	8 (11%)	0 (0%)	
6	27 (38%)	10 (25%)	0.0058 [†]
7	34 (47%)	26 (65%)	
8	2 (3%)	3 (8%)	0.036 [‡]
9	1 (1%)	1 (2%)	
pStage			
T _{1b}	0 (0%)	1 (2%)	
T _{2a}	12 (17%)	3 (8%)	0.0185 [†]
T _{2b}	41 (57%)	17 (42%)	
T _{3a}	16 (22%)	12 (30%)	0.031 [†]
T _{3b}	3 (4%)	7 (18%)	
Race			
White	67 (93%)	35 (88%)	0.2224 [†]
Black	3 (5%)	2 (5%)	
Other	1 (1%)	3 (7%)	0.385 [†]
Unknown	1 (1%)	0 (0%)	

*Median test.

[†] Wilcoxon's rank-sum test.

[‡] Fisher's exact test.

Table 3. QNG signature

NMD	Measurement type	β Coefficient	$P > z$
Area	Size and shape	-0.0490319	0.004
SD Gray values	DNA content	-0.0762125	0.010
Intensity	DNA content	6.07E-09	0.010
Skewness of OD	DNA content	5.849436	0.048
Excess of OD	DNA content	-0.0249485	0.034
DNA ploidy	DNA content	17.29464	0.001
Sum mean	Texture	2603.313	0.021
Sum entropy	Texture	-11225.53	0.024
Cluster shade	Texture	0.0270699	0.012
Sum of homogeneity	Texture	-29869.61	0.017
Correlation	Markovian	-643.6912	0.037
Inverse difference moment	Markovian	41413.18	0.018
Peak transition probability	Markovian	16359.42	0.048
Second diagonal moment	Markovian	-838.5605	0.013
Logistic regression model constant		4.213619	0.039

of 0.34 for the predictive probabilities, the sensitivity, specificity, and accuracy of the LR model were 75%, 78%, and 77%, respectively (Fisher's exact $P < 0.001$). Figure 4B shows a scatter plot of the patient-specific predictive probabilities from the combined model for patients with and without biochemical recurrence. It is interesting to note that by combining the pathology variables with the QNG signature, there was not a statistically significant increase in the AUC-ROC compared with the use of the QNG signature alone ($\chi^2 P = 0.3380$).

Table 4A and B shows a comparison of the predictive abilities of the three different models. Table 4A compares the predictive probability threshold, specificity, positive predictive value (PPV), negative predictive value (NPV), and accuracy of the models at sensitivities of ~90%, 95%, and 100%. Table 4B compares the predictive probability threshold, sensitivity, PPV, NPV, and accuracy of the models at specificities of ~90%, 95%, and 100%. These tables show that a QNG signature is able to differentiate between patients with and without biochemical recurrence much better than the pathology variables alone, and that the combination of the QNG and pathology variables does not improve the prognostic discrimination in this patient cohort.

We also assessed the abilities of the QNG signature alone, the pathology variables alone, and the combination of the two to predict the PSA recurrence-free survival after radical prostatectomy for the 112 men in the CPCTR patient cohort using Kaplan-Meier plots and Cox proportional hazards regression. Figure 5 shows that patients with a favorable QNG value of <0.39 have significantly longer PSA recurrence-free survival times compared with those with an unfavorable QNG value of ≥ 0.39 (>12 years versus 3.4 years; log-rank $P < 0.0001$; Cox hazard ratio, 6.1). The proportion of patients with biochemical recurrence in the favorable and unfavorable QNG groups was also significantly different (16% versus 63%, respectively, Fisher's exact $P < 0.001$).

Figure 6 illustrates that patients with favorable pathology variables (pathology model predictive probability <0.35) have a significantly longer PSA recurrence-free survival time compared with those with unfavorable pathology variables (pathology model predictive probability ≥ 0.35 ; >12 years versus 7.0 years; log-rank $P = 0.0162$; Cox hazard ratio, 2.2). The proportion of patients with biochemical recurrence in

the favorable and unfavorable pathology groups was also significantly different (25% versus 44%, respectively, Fisher's exact $P = 0.048$). The significant difference in prognostic performance between QNG and the

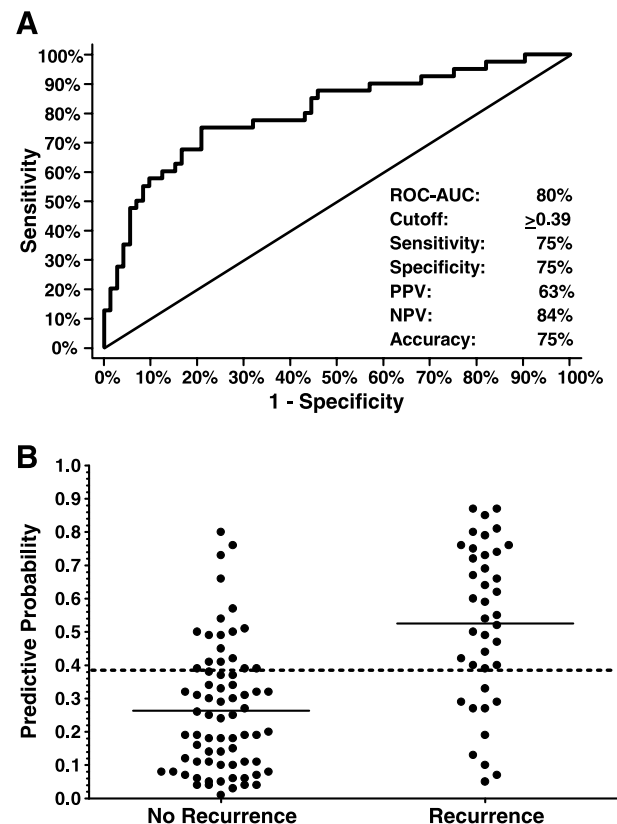


Figure 2. A. ROC curve for the ability of the QNG signature to predict biochemical recurrence using a multivariate logistic regression model of 14 different NMDs. The AUC-ROC and the sensitivity, specificity, PPV, NPV, and accuracy for the specified predictive probability cutoff are also provided. B. Scatter plot of the predictive probabilities for the patients with and without biochemical recurrence. Solid lines, mean values in each group; dotted line, the cutoff used to identify patients with a favorable QNG signature (predictive probability <0.39) and those with an unfavorable QNG signature (predictive probability ≥ 0.39).

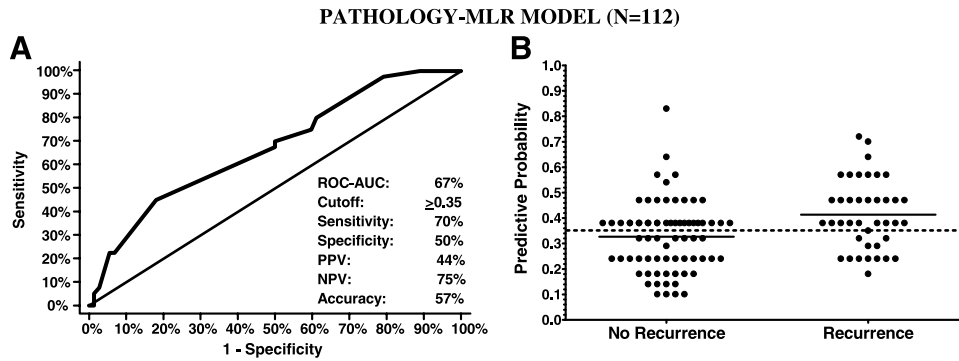


Figure 3. **A.** ROC curve for the ability of the combined pathology variables (Gleason score and pathologic stage) to predict biochemical recurrence. The AUC-ROC and the sensitivity, specificity, PPV, NPV, and accuracy for the specified predictive probability cutoff are also provided. **B.** Scatter plot of the predictive probabilities for the patients with and without biochemical recurrence. *Solid lines*, mean values in each group; *dotted line*, the cutoff used to identify patients with favorable pathology (predictive probability <0.35) and those with an unfavorable pathology (predictive probability ≥ 0.35).

pathology variables is further illustrated by comparing the Cox hazard ratios of 6.1 for QNG (95% confidence interval, 3.0-12.6) versus 2.2 (95% confidence interval, 1.1-4.4) for pathology (Figs. 5 and 6).

When QNG was combined with the Gleason score and pathologic stage, the predictive ability was nearly identical to that of QNG alone. Patients with a favorable combined model value (combined model predictive probability <0.34) had a significantly longer PSA recurrence-free survival time compared with those with an unfavorable combined model value (combined model predictive probability ≥ 0.34) (>12 years versus 3.2 years; log-rank $P < 0.0001$; Cox hazard ratio, 6.3).

Discussion

The prospect of recurrence determined by PSA monitoring produces a constant fear in men diagnosed and definitively treated for prostate cancer by either surgery or irradiation. The definition of recurrence is often based

on a PSA nadir for which the kinetics of achievement differs for men that undergo radical prostatectomy versus radiation (24-26). Because PSA levels can be tracked fairly reliably over time, the finding of increased serum PSA concentrations is considered evidence of disease recurrence and hence is an intervention determinant for a prostate cancer patient (4-11, 24).

Long-term follow-up of men definitively treated for prostate cancer has revealed up to a 30% to 40% risk for a PSA recurrence and is cause for therapeutic intervention within 10 years posttreatment (4-11, 24-27). Studies by Pound et al. (3) and Han et al. (4) of ~2,000 prostate cancer patients treated by radical prostatectomy determined that the incidence of biochemical recurrence was 15% and 17%, respectively, and that the distant metastasis in these groups was ~34%. Han et al. (4) showed that PSA recurrence-free survival at 5, 10, and 15 years was 84%, 72%, and 61%, respectively, and they calculated separate nomograms to stratify by preoperative clinical stages pT_{1c} , pT_{2a} , $pT_{2b/c}$ and postoperative organ

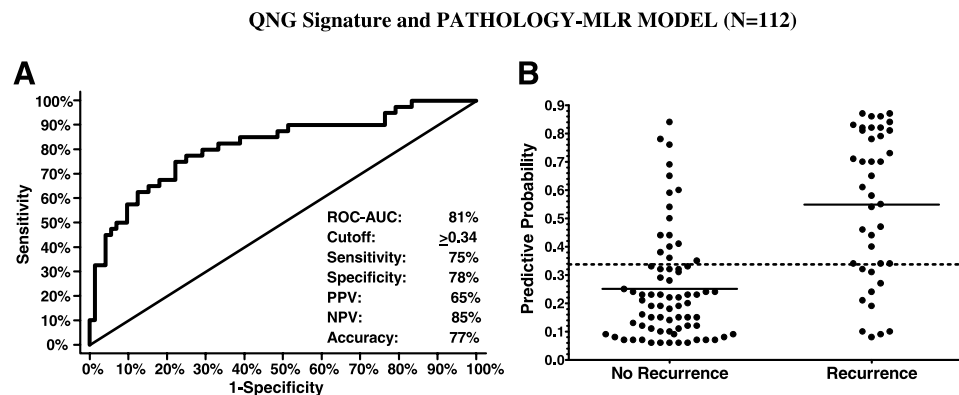


Figure 4. **A.** ROC curve for the ability of the pathology variables and the QNG signature combined to predict biochemical recurrence. The AUC-ROC and the sensitivity, specificity, PPV, NPV, and accuracy for the specified predictive probability cutoff are also provided. **B.** Scatter plot of the predictive probabilities for the patients with and without biochemical recurrence. *Solid lines*, mean values in each group; *dotted line*, the cutoff used to identify patients with a favorable predictive probability (<0.34) and those with an unfavorable predictive probability (≥ 0.34).

Table 4. Summary of LR models for prediction of biochemical recurrence-free survival

A. Specificity at common sensitivity									
AUC-ROC	QNG			Pathology			QNG + pathology		
	80%			67%			81%		
Threshold (\geq)	0.19	0.10	0.05	0.29	0.24	0.18	0.19	0.10	0.08
Sensitivity	90%	95%	100%	80%	98%	100%	90%	95%	100%
Specificity	42%	22%	8%	39%	21%	11%	44%	22%	15%
PPV	46%	40%	38%	42%	41%	38%	47%	40%	40%
NPV	88%	89%	100%	78%	94%	100%	89%	89%	100%
Accuracy	59%	48%	41%	54%	48%	43%	61%	48%	46%

B. Sensitivity at common specificity									
AUC-ROC	QNG			Pathology			QNG + pathology		
	80%			67%			81%		
Threshold (\geq)	0.51	0.58	0.81	0.48	0.55	0.84	0.55	0.69	0.81
Sensitivity	55%	48%	10%	23%	23%	0%	55%	45%	10%
Specificity	90%	94%	100%	93%	94%	100%	90%	94%	100%
PPV	76%	83%	100%	64%	69%	0%	76%	82%	100%
NPV	78%	76%	67%	68%	69%	64%	78%	76%	67%
Accuracy	78%	78%	68%	68%	69%	64%	78%	77%	68%

confined and nonorgan confined disease. Khan et al. (27) determined the probability of PSA-free disease at 5 and 10 years in 1,955 men treated for localized prostate cancer based on using Gleason score, pathologic stage, and surgical margin status. They created four categories of risk based on these three postoperative criteria, and the PSA recurrence-free survival at 10 years in these risk groups ranged from 95% to 13%. Kattan et al. (28) developed a nomogram, based on Cox hazards modeling of PSA, clinical stage, and Gleason grade, yielding a AUC-ROC of 0.76; however, the model only predicted 5-year PSA recurrence-free survival probabilities. Stephenson et al. (29) developed a postoperative prostate cancer nomogram using PSA, 1^o Gleason grade, 2^o

Gleason grade, extracapsular extension, positive surgical margins, seminal vesicle invasion, lymph node involvement, treatment year, and adjuvant radiotherapy, which predicted 10-year PSA recurrence-free survival probabilities and had a concordance index of 0.81. Cooperberg et al. (30) established the University of California at San Francisco cancer of the Prostate Risk Assessment based on an evaluation of 1,439 prostate cancer cases having 219 (15%) biochemical PSA recurrences. Their University of California at San Francisco cancer of the Prostate Risk Assessment algorithm combines scores for PSA (0-4), Gleason sum (0-3), pathologic stage (0-1), age (0-1), and percent of positive cores on the biopsy (0-1) to generate a CAPRA score that predicts 5-year biochemical

Ability of the QNG signature to Predict Biochemical Recurrence Free Survival in Men (N=112) Treated by Radical Prostatectomy

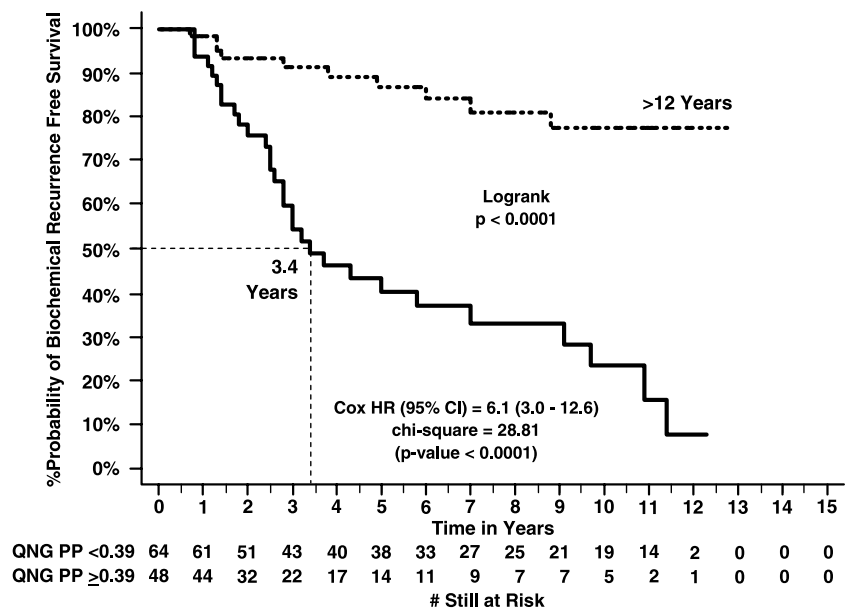


Figure 5. Kaplan-Meier curve comparing the biochemical recurrence-free survival in patients with a favorable QNG signature (predictive probability <0.39) with those having an unfavorable QNG signature (predictive probability \geq 0.39). The survival curves were compared using the log-rank test. Median biochemical recurrence-free survival times with 95% confidence intervals are also presented, as well as the results of a Cox proportional hazards regression.

Ability of routine pathology to Predict Biochemical Recurrence Free Survival in N=112 Men Treated with Radical Prostatectomy

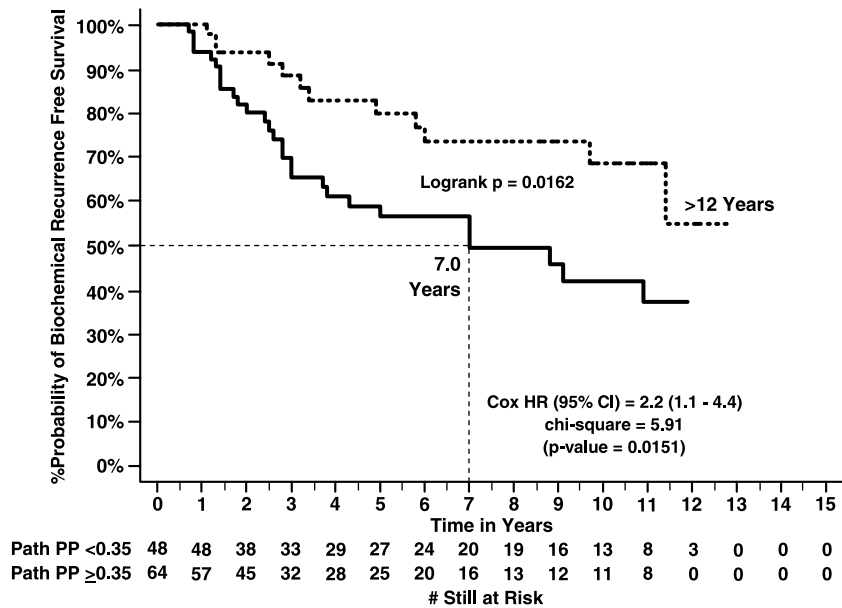


Figure 6. Kaplan-Meier curve comparing the biochemical recurrence-free survival in patients with favorable pathology (predictive probability <0.35) with those having unfavorable pathology (predictive probability ≥0.35). The survival curves were compared using the log-rank test. Median biochemical recurrence-free survival times with 95% confidence intervals are also presented, as well as the results of a Cox proportional hazards regression.

recurrence-free survival probabilities and has a concordance index of 0.66 (30). The clinical value of PSA as a prognostic biomarker has been well illustrated by Freedland et al. (31) when they determined 10-year PSA recurrence-free probabilities in 2,312 prostate cancer patients and used pretreatment PSA stratified by five categories ranging from 2.0 to 9.9 ng/mL to determine risk for biochemical recurrence. D’Amico et al. (32) used preoperative PSA velocity at a cutoff of 2.0 ng/mL/y and postoperative PSA doubling time at cutoffs of <3 months (high risk) or >12 months (low risk) to predict clinically insignificant PSA recurrence risk. Recently, Cordon-Cardo et al. (33) used domain expertise machine learning, which include knowledge of biomarker stratification and image analysis with support vector regression for censored data, to generate a predictive model. They selected four clinicopathologic, three morphometric, and one molecular feature from an initial set of 93 features. The combined model predicted biochemical recurrence with high accuracy, as indicated by a concordance index in the validation set of 0.82, with a sensitivity of 96% and a specificity of 72%. PSA was not used in this multivariate machine support vector model. When the Kattan nomogram (29) that did use PSA was applied to this same prostate cancer cohort (33), the model had a concordance index of only 0.71 compared with 0.81 as reported by Kattan in 2005.

A significant weakness of this study was the lack of available preoperative serum PSA measurements on all the *n* = 112 prostate cancer cases and hence an inability to use total PSA as a continuous variable. In the future, investigators who wish to use the NCI-CPCTR TMA⁵ resource must be aware that there are only 112 of 299

prostate cancer cases that have verifiable PSA recurrence documented based on the criteria used to assess this event. Therefore, to our disadvantage, we could not use total PSA as a preoperative test variable for our multivariable logistic regression models.

However, others have shown that PSA is not significantly correlated with biochemical failure after radical prostatectomy for larger volume cancers (6 mL or greater), for patients with PSA <10 ng/mL, or for transitional zone cancer (34-36). Another limitation of our study is that the sample size is small. However, our approach has been to construct models for assessment of biochemical recurrence and disease progression using routine pretreatment clinical and postoperative pathology variables, and to compare these to models where the new biomarkers are added. The resulting combined models are tested to determine if such modifications result in statistically and clinically significant improvements of the predictive and prognostic abilities of the current standards (37, 38). Ultimately, however, testing of such new computational models must be done on larger numbers of unknown cases retrospectively and then applied prospectively to validate an algorithm’s clinical utility in assisting the physician and patient to make informed decisions about intervention.

Our method applied multivariate logistic regression to calculate a QNG signature using ~125 randomly selected Feulgen DNA-stained nuclei from cancer areas on a NCI-CPCTR TMA. This QNG model had an AUC-ROC of 80% with a sensitivity, specificity, and accuracy of 75% for the differentiation of patients with and without biochemical recurrence and was more accurate than the use of pathology (Gleason score and pathologic stage), which showed a sensitivity of 70%, a specificity of 50%, and an accuracy of 57%. Combining the QNG signature with pathology (Gleason score and stage) resulted in a small but insignificant increase in the

⁵ <http://cpctr.cancer.gov>

specificity and accuracy compared with only the QNG signature (Table 4). The biochemical (PSA)-free survival prognostic performances of these models, shown in the Kaplan-Meier plots illustrated in Figs. 5 and 6, also showed that the use of the QNG signature alone was superior to the use of the pathology variables and that it was not significantly different when the two were combined.

It is important to ultimately understand the molecular basis of alterations in nuclear structure that determine clinical risk for disease recurrence and progression to distant metastasis. Toward this end, Debes et al. (39) have already shown that P300 (histone acetyltransferase) overexpression correlates specifically to nuclear alterations of size and shape using prostate cancer cell lines transformed with the *P300* gene. Seligson et al. (40) have shown that molecularly modified histones H3 and H4 correlate with PSA recurrence; however, the correlation with nuclear structure alterations has not been made. More recently, our laboratory reported at the AACR meeting held in Washington, DC, from April 1 to 5, 2006, on the QNG signature for the CPCTR-TMA and also showed that such *P300* protein overexpression correlates to a shape parameter in PSA recurrence (41). Future research involves collaboration with Dr. David Seligson at University of California at Los Angeles and a long-term follow-up cohort of 247 men to validate our NCI-CPCTR findings on the use of a nuclear morphometry algorithm alone and also to enhance the model for predicting biochemical recurrence after radical prostatectomy using nuclear morphometry, clinical variables, and other histologic biomarkers of progression. Clearly, a better understanding of the molecular modifications that control nuclear structure should provide new molecular targets for diagnosis and treatment of prostate cancer as well as improved knowledge of mechanisms of carcinogenesis.

In conclusion, nuclear morphometric signatures can be used to make predictions of biochemical-free survival in men that have undergone surgical treatment for their prostate cancer. Such signatures can be combined with routine pathology, PSA derivative analysis, and other new biomarkers to produce even more precise models (12, 19, 37, 38). Early prediction of a patient's risk for disease progression (i.e., recurrence) based on morphologic and molecular biomarkers may permit the development of new and innovative intervention strategies such as chemoprevention and/or other adjuvant therapies.

References

- Walsh PC. Anatomic radical prostatectomy: evolution of the surgical technique. *J Urol* 1998;160:2418–24.
- Walsh PC, Donker PJ. Impotence following radical prostatectomy: insight into etiology and prevention. *J Urol* 1982;128:492–7.
- Pound CR, Partin AW, Eisenberger MA, Chan DW, Pearson JD, Walsh PC. Natural history of progression after PSA elevation following radical prostatectomy. *JAMA* 1999;281:1591–7.
- Han M, Partin AW, Zahurak M, Piantadosi S, Epstein JI, Walsh PC. Biochemical (prostate specific antigen) recurrence probability following radical prostatectomy for clinically localized prostate cancer. *J Urol* 2003;169:517–23.
- Catalona WJ, Smith DS. 5-year tumor recurrence rates after anatomical radical retropubic prostatectomy for prostate cancer. *J Urol* 1994;152:1837–42.
- Catalona WJ, Smith DS. Cancer recurrence and survival rates after anatomic radical retropubic prostatectomy for prostate cancer: intermediate-term results. *J Urol* 1998;160:2428–34.
- Ohori M, Goad JR, Wheeler TM, Eastham JA, Thompson TC, Scardino PT. Can radical prostatectomy alter the progression of poorly differentiated prostate cancer? *J Urol* 1994;152:1843–9.
- Trapasso JG, deKernion JB, Smith RB, Dorey F. The incidence and significance of detectable levels of serum prostate specific antigen after radical prostatectomy. *J Urol* 1994;152:1821–5.
- Freedland SJ, Presti JC, Jr., Amling CL, et al. Time trends in biochemical recurrence after radical prostatectomy: results of the SEARCH database. *Urology* 2003;61:736–41.
- Freedland SJ, Humphreys EB, Mangold LA, et al. Risk of prostate cancer-specific mortality following biochemical recurrence after radical prostatectomy. *JAMA* 2005;294:433–9.
- Ward JF, Moul JW. Rising prostate-specific antigen after primary prostate cancer therapy. *Nat Clin Pract* 2005;2:174–82.
- Veltri RW. Molecular biology of serum biomarkers of prostate cancer. In: Kirby RS, Partin AW, Feneley MR, Parsons JK, editors. *Prostate cancer: Principles and Practice*. London & New York: Taylor & Francis; 2006. p. 269–84.
- Tricoli JV, Schoenfeldt M, Conley BA. Detection of prostate cancer and predicting progression: current and future diagnostic markers. *Clin Cancer Res* 2004;10:3943–53.
- Bacus JW, Grace LJ. Optical microscope system for standardized cell measurements and analyses. *Appl Opt* 1987;26:3280–93.
- Veltri RW, Partin AW, Miller MC. Quantitative nuclear grade (QNG): a new image analysis-based biomarker of clinically relevant nuclear structure alterations. *J Cell Biochem* 2000;Suppl 35:151–7.
- Veltri RW, Partin AW, Epstein JE, et al. Quantitative nuclear morphometry, Markovian texture descriptors, and DNA content captured on a CAS-200 Image analysis system, combined with PCNA and HER-2/neu immunohistochemistry for prediction of prostate cancer progression. *J Cell Biochem* 1994;19:249–58.
- Cairns P, Sidransky D. Molecular methods for the diagnosis of cancer. *Biochim Biophys Acta* 1999;1423:C11–8.
- Stein GS, Montecino M, van Wijnen AJ, Stein JL, Lian JB. Nuclear structure-gene expression interrelationships: implications for aberrant gene expression in cancer. *Cancer Res* 2000;60:2067–76.
- Veltri RW, Partin AW, Miller CM. Quantitative nuclear grade (QNG): the clinical applications of the quantitative measurement of nuclear structure using image analysis. In: Kelloff GJ, Hawk ET, Sigman CC, editors. *Cancer chemoprevention*. Totowa (NJ): Humana Press; 2005. p. 97–108.
- Melamed J, Datta MW, Becich MJ, et al. The cooperative prostate cancer tissue resource: a specimen and data resource for cancer researchers. *Clin Cancer Res* 2004;10:4614–21.
- Berman JJ, Datta M, Kajdacsy-Balla A, et al. The tissue microarray data exchange specification: implementation by the Cooperative Prostate Cancer Tissue Resource. *BMC Bioinformatics* 2004;5:19.
- Patel AA, Kajdacsy-Balla A, Berman JJ, et al. The development of common data elements for a multi-institute prostate cancer tissue bank: the Cooperative Prostate Cancer Tissue Resource (CPCTR) experience. *BMC Cancer* 2005;5:108.
- Liao Z, Datta MW. A simple computer program for calculating PSA recurrence in prostate cancer patients. *BMC Urol* 2004;4:8.
- Partin AW, Pound CR, Clemens JQ, Epstein JI, Walsh PC. Serum PSA after anatomic radical prostatectomy. The Johns Hopkins experience after 10 years. *Urol Clin North Am* 1993;20:713–25.
- Chodak GW, Neumann J, Blix G, Sutton H, Farah R. Effect of external beam radiation therapy on serum prostate-specific antigen. *Urology* 1990;35:288–94.
- Cadeddu JA, Pearson JD, Partin AW, Epstein JI, Carter HB. Relationship between changes in prostate-specific antigen and prognosis of prostate cancer. *Urology* 1993;42:383–9.
- Khan MA, Partin AW, Mangold LA, Epstein JI, Walsh PC. Probability of biochemical recurrence by analysis of pathologic stage, Gleason score, and margin status for localized prostate cancer. *Urology* 2003;62:866–71.
- Kattan MW, Eastham JA, Stapleton AM, Wheeler TM, Scardino PT. A preoperative nomogram for disease recurrence following radical prostatectomy for prostate cancer. *J Natl Cancer Inst* 1998;90:766–71.
- Stephenson AJ, Scardino PT, Eastham JA, et al. Postoperative nomogram predicting the 10-year probability of prostate cancer recurrence after radical prostatectomy. *J Clin Oncol* 2005;23:7005–12.
- Cooperberg MR, Pasta DJ, Elkin EP, et al. The University of California, San Francisco Cancer of the Prostate Risk Assessment score: a straightforward and reliable preoperative predictor of disease recurrence after radical prostatectomy. *J Urol* 2005;173:1938–42.
- Freedland SJ, Mangold LA, Walsh PC, Partin AW. The prostatic

- specific antigen era is alive and well: prostatic specific antigen and biochemical progression following radical prostatectomy. *J Urol* 2005;174:1276–81; discussion 81; author reply 81.
32. D'Amico AV, Chen MH, Roehl KA, Catalona WJ. Identifying patients at risk for significant versus clinically insignificant postoperative prostate-specific antigen failure. *J Clin Oncol* 2005;23:4975–9.
 33. Cordon-Cardo C, Kotsianti A, Verbel DA, et al. Improved prediction of prostate cancer recurrence through systems pathology. *J Clin Invest* 2007;117:1876–83.
 34. Noguchi M, Stamey TA, McNeal JE, Yemoto CM. Preoperative serum prostate specific antigen does not reflect biochemical failure rates after radical prostatectomy in men with large volume cancers. *J Urol* 2000;164:1596–600.
 35. Stamey TA. Preoperative serum prostate-specific antigen (PSA) below 10 microg/l predicts neither the presence of prostate cancer nor the rate of postoperative PSA failure. *Clin Chem* 2001;47:631–4.
 36. Stamey TA, Yemoto CM, McNeal JE, Sigal BM, Johnstone IM. Prostate cancer is highly predictable: a prognostic equation based on all morphological variables in radical prostatectomy specimens. *J Urol* 2000;163:1155–60.
 37. Kattan MW. Judging new markers by their ability to improve predictive accuracy. *J Natl Cancer Inst* 2003;95:634–5.
 38. Kattan MW. Evaluating a new marker's predictive contribution. *Clin Cancer Res* 2004;10:822–4.
 39. Debes JD, Sebo TJ, Heemers HV, et al. p300 modulates nuclear morphology in prostate cancer. *Cancer Res* 2005;65:708–12.
 40. Seligson DB, Horvath S, Shi T, et al. Global histone modification patterns predict risk of prostate cancer recurrence. *Nature* 2005;435:1262–6.
 41. Marlow C, Makarov DV, Miller MC, Partin AW, Veltri RW. Improved prediction of PSA biochemical recurrence by quantitative nuclear grade (QNG) using the NCI CPCTR-prostate tissue microarray. *AACR Meeting Abstracts*, April 2006;47:1242.